

Pressure and Temperature Dependence of the Dielectric Properties and Phase Transitions of the Antiferroelectric Perovskites: PbZrO_3 and PbHfO_3 †

G. A. SAMARA

Sandia Laboratories, Albuquerque, New Mexico 87115

(Received 19 June 1969; revised manuscript received 8 January 1970)

Hydrostatic-pressure measurements have shown that in PbZrO_3 the antiferroelectric (AFE)-paraelectric (PE) transition temperature T_a increases ($dT_a/dP = 4.5 \pm 0.3^\circ\text{K/kbar}$), whereas the extrapolated Curie-Weiss temperature T_0 decreases ($dT_0/dP = -16.0 \pm 0.5^\circ\text{K/kbar}$) with increasing pressure. Interpreted in terms of the lattice dynamics, the results give the first experimental evidence that there are two independent low-frequency temperature-dependent lattice vibrational modes in PbZrO_3 : a ferroelectric (FE) mode which determines the large polarizability and the Curie-Weiss behavior of the static dielectric constant in the paraelectric phase, and an AFE mode (probably a coupled mode) which causes the AFE transition. On cooling, the crystal becomes unstable against the AFE mode at T_a just before the instability due to the FE mode is reached at T_0 . Pressure increases the frequency of the FE mode but decreases ("softens") that of the AFE mode, and consequently, the static-dielectric-constant anomaly at the transition decreases sharply. The behavior of PbHfO_3 is qualitatively similar to that of PbZrO_3 , but is complicated by the presence of two AFE phases at 1 bar. A third AFE phase becomes stable at high pressure. All the AFE transition temperatures increase with pressure, corresponding to the softening of their respective AFE modes. A brief discussion of the nature of the AFE mode in PbZrO_3 is given.

I. INTRODUCTION AND THEORETICAL BACKGROUND

THE nature of the phase transitions exhibited by substances crystallizing in the cubic perovskite structure and the interpretation of these transitions in terms of instabilities of certain normal modes of vibration have received much recent interest.¹⁻⁶ Specifically, the transition to the ferroelectric (FE) state in perovskites such as BaTiO_3 has now been correlated both theoretically⁷ and experimentally⁶ with the existence of a low-frequency temperature-dependent, transverse optical (TO) mode at the center of the Brillouin zone (i.e., zero wave vector \mathbf{q}). The observed Curie-Weiss temperature dependence of the static dielectric constant in the high-temperature paraelectric (PE) phase, i.e.,

$$\epsilon = C/(T - T_0), \quad (1)$$

is associated with the softening of the frequency (ω_f) of this so-called FE mode according to

$$\omega^2(\mathbf{q}=0, j_1) \equiv \omega_f^2 = K(T - T_0). \quad (2)$$

In Eqs. (1) and (2), T_0 is the extrapolated Curie-Weiss temperature, j_1 designates the pertinent TO branch, and C and K are constants. Formally, Eqs. (1) and (2)

are related (in the absence of, or for small damping of the modes) through the generalized Lyddane-Sachs-Teller (LST) relationship

$$\epsilon/\epsilon_\infty = \prod_i [(\omega_L)_i^2/(\omega_T)_i^2]. \quad (3a)$$

In Eq. (3a), ϵ_∞ is the high-frequency, or optical, dielectric constant ($=n^2$, where n is the refractive index), and ω_L and ω_T are the longitudinal and transverse optic phonon frequencies for the various modes. Cochran⁷ pointed out that it is necessary that the frequency of only *one* mode $\rightarrow 0$ as $T \rightarrow T_0$,⁸ and, indeed, it is now established that in many perovskites, including BaTiO_3 ,⁶ SrTiO_3 ,^{9,10} and KTaO_3 ,^{10,11} nearly all of the T dependence of the phonon frequencies arises from a single TO phonon, the lowest frequency or the FE mode. Thus, Eq. (3a) can be rewritten as

$$\omega_f^2 \epsilon = \epsilon_\infty \left[\prod_i (\omega_L)_i^2 / \prod_i' (\omega_T)_i^2 \right] = A, \quad (3b)$$

where the product \prod_i' is taken over all the TO frequencies except ω_f , and A is a constant. Experimentally, the T dependence $\omega_f^2(T) = A/\epsilon(T)$ has been verified,^{6,9-11} and, furthermore, the absolute value of A is quite accurately given¹⁰ by the middle term of Eq. (3b).

Cochran⁷ has suggested that a transition to an antiferroelectric (AFE) state can be associated with an instability of another mode(s) whose wavelength is on the order of a lattice parameter (i.e., a zone-boundary mode). The temperature dependence of the frequency

⁸ It is not necessary that the frequency of this mode vanish precisely at the actual transition.

⁹ R. A. Cowley, Phys. Rev. **134**, A981 (1964).

¹⁰ P. A. Fleury and J. M. Worlock, Phys. Rev. **174**, 613 (1968).

¹¹ G. Shirane, R. Nathans, and V. J. Minkiewicz, Phys. Rev. **157**, 396 (1967).

† Work supported by the U. S. Atomic Energy Commission.

¹ K. A. Müller, W. Berlinger, and F. Waldner, Phys. Rev. Letters **21**, 814 (1968).

² P. A. Fleury, J. F. Scott, and J. M. Worlock, Phys. Rev. Letters **21**, 16 (1968).

³ W. Cochran and A. Zia, Phys. Status Solidi **25**, 273 (1968).

⁴ G. Shirane and Y. Yamada, Phys. Rev. **177**, 858 (1969); see also *ibid.* **183**, 820 (1969).

⁵ V. J. Minkiewicz and G. Shirane, Bull. Am. Phys. Soc. **13**, 1376 (1968).

⁶ Y. Yamada, G. Shirane, and A. Linz, Phys. Rev. **177**, 848 (1969); see also G. Shirane *et al.*, Phys. Rev. Letters **19**, 234 (1967).

⁷ W. Cochran, Advan. Phys. **9**, 387 (1960); **10**, 401 (1961).

TABLE I. Values of the transition parameters for PbZrO_3 and PbHfO_3 . T_t is the transition temperature at 1 bar, and ΔV and Q are the accompanying volume change and transition heat, respectively. Experimental values for the pressure derivative of T_t are compared with values calculated from the Clausius-Clapeyron equation where the necessary data are available. Corresponding quantities for BaTiO_3 and PbTiO_3 (taken from Ref. 29) are listed for comparison.

Substance	Transition	T_t (°K)	ΔV (Å ³ /cell)	Q (Cal/mole)	$(dT_t/dP)_{\text{expt.}}$ (°K/kbar)	$(dT_t/dP)_{\text{calc.}}$ (°K/kbar)
PbZrO_3	AFE \rightarrow PE	507	0.29 ± 0.02^a	$\sim 420 \pm 20^b$	4.5 ± 0.3	5.0 ± 0.7
PbHfO_3	AFE(δ) \rightarrow AFE(γ)	434	0.27 ^c	$(290 \pm 30)^d$	5.9 ± 0.6	...
	AFE(γ) \rightarrow AFE(β)	476 ^e	5.0 ± 0.5	...
	AFE(β) \rightarrow PE(α)	476	14.3 ± 1.0	...
BaTiO_3	FE \rightarrow PE	393	-0.06	~ 50	-5.5 ± 1.0	-7.0
PbTiO_3	FE \rightarrow PE	760	-0.27	~ 1150	< -8	-2.6

^a Estimated from data in Refs. 16, 18, and 19.

^b From Ref. 16.

^c From Ref. 20.

^d Calculated from Eq. (5) using the experimental value of dT_t/dP .

^e Value based on the extrapolation of the β - γ phase boundary to zero pressure.

(ω_a) of this AFE mode can be written as¹²

$$\omega^2(\mathbf{q} \neq 0, j_2) \equiv \omega_a^2 \alpha K'(T - T_a), \quad (4)$$

where T_a is the AFE transition temperature and K' is a constant. Unfortunately, due to the lack of suitable single crystals, the dispersion curves and their temperature dependence have not been measured for any of the well-known AFE perovskites such as lead zirconate, PbZrO_3 .¹³

Experimentally, an interesting situation is observed in PbZrO_3 (and also in PbHfO_3 and NaNbO_3), and certain theoretical aspects of the antiferroelectricity of this material have been treated recently.^{3,14} The crystal transforms from the high-temperature cubic PE phase to an orthorhombic AFE phase at $\sim 505^\circ\text{K}$. In the PE phase, the dielectric constant ϵ obeys the Curie-Weiss law, Eq. (1), with $T_0 \approx 475^\circ\text{K}$, and there is a large anomaly in ϵ ($\epsilon_{\text{max}} \approx 5000$) at the AFE transition.

Since according to the LST relationship, a large ϵ must always be associated with the existence of a low-frequency ($\mathbf{q}=0$) TO mode (i.e., a FE mode), the above behavior strongly suggests that in PbZrO_3 there are two low-frequency temperature-dependent modes: a FE mode which determines the large polarizability and an AFE mode which causes the transition. On lowering the temperature, the crystal becomes unstable against the AFE mode at T_a just before the instability due to the FE mode is reached at T_0 .

In this paper we present the first experimental evidence that the large dielectric anomaly at the AFE transition and the transition itself in PbZrO_3 are indeed determined by two independent modes. The evidence

¹² There is no simple theoretical explanation for this indicated linear T dependence of ω_a^2 [see W. Cochran, *Advan. Phys.* **18**, 157 (1969)]. Experimental justification for Eq. (4) has come from measurements on the soft, zone-boundary mode (Γ_{25}) in SrTiO_3 , KMnF_3 , and LaAlO_3 (Refs. 4 and 5).

¹³ As will be pointed out later, the softening of a zone boundary mode (Γ_{25}) has been definitely established (Refs. 1-5) as the cause of the transitions in SrTiO_3 , KMnF_3 , and LaAlO_3 ; however, none of these transitions is to an AFE state. Here we adopt Jona and Shirane's definition for antiferroelectricity [F. Jona and G. Shirane, *Ferroelectric Crystals* (Macmillan, New York, 1962), p. 23].

¹⁴ P. B. Miller and P. C. Kwok, *Solid State Commun.* **5**, 57 (1967).

is based on measurements of the effects of temperature and hydrostatic pressure on the dielectric properties of PbZrO_3 . An analogous situation occurs in PbHfO_3 , and this substance was studied also. An added feature of the results is that in addition to the two AFE phases which are known to occur in PbHfO_3 , a third AFE phase becomes stable at high pressure. In the next section we review briefly the crystallographic and dielectric properties of PbZrO_3 and PbHfO_3 observed at atmospheric pressure and mention earlier pressure studies. The following sections describe the experimental details and present the results and their interpretation.

II. CRYSTALLOGRAPHIC AND DIELECTRIC PROPERTIES AT ATMOSPHERIC PRESSURE AND EARLIER PRESSURE STUDIES

The low-temperature AFE phase of PbZrO_3 has orthorhombic symmetry (space group $\text{Pba}2\text{-C}_{2v}$)⁸ with eight molecules per unit cell.¹⁵ This phase has been often described as pseudotetragonal with $c/a = 0.988$. On heating it transforms at $\sim 500^\circ\text{K}$ to a paraelectric (PE) phase having the cubic perovskite structure (space group $\text{Pm}3m\text{-O}_h$). The transition is first-order accompanied by a discontinuous volume change and a latent heat. Some of the transition parameters are summarized in Table I.

There is considerable evidence that an intermediate FE phase occurs in *some* samples of PbZrO_3 over a rather narrow temperature range. The early measurements of Sawaguchi *et al.*¹⁶ showed a single transition at 497°K on heating and two transitions at 496 and 476°K on cooling. The phase between the two latter temperatures was found to be ferroelectric with rhombohedral symmetry ($c/a > 1$). The authors attributed the appearance of this intermediate phase to the presence of impurities in their samples, and, indeed, it is now well established^{16,17} that small amounts of Ti, V, Nb, Ta, etc. stabilize this FE phase.

¹⁵ F. Jona, G. Shirane, F. Mazzi, and R. Pepinsky, *Phys. Rev.* **105**, 849 (1957).

¹⁶ E. Sawaguchi, G. Shirane, and Y. Takagi, *J. Phys. Soc. Japan* **6**, 333 (1951); **7**, 110 (1952).

¹⁷ L. Benguigui, *Compt. Rend.* **267B**, 928 (1968).

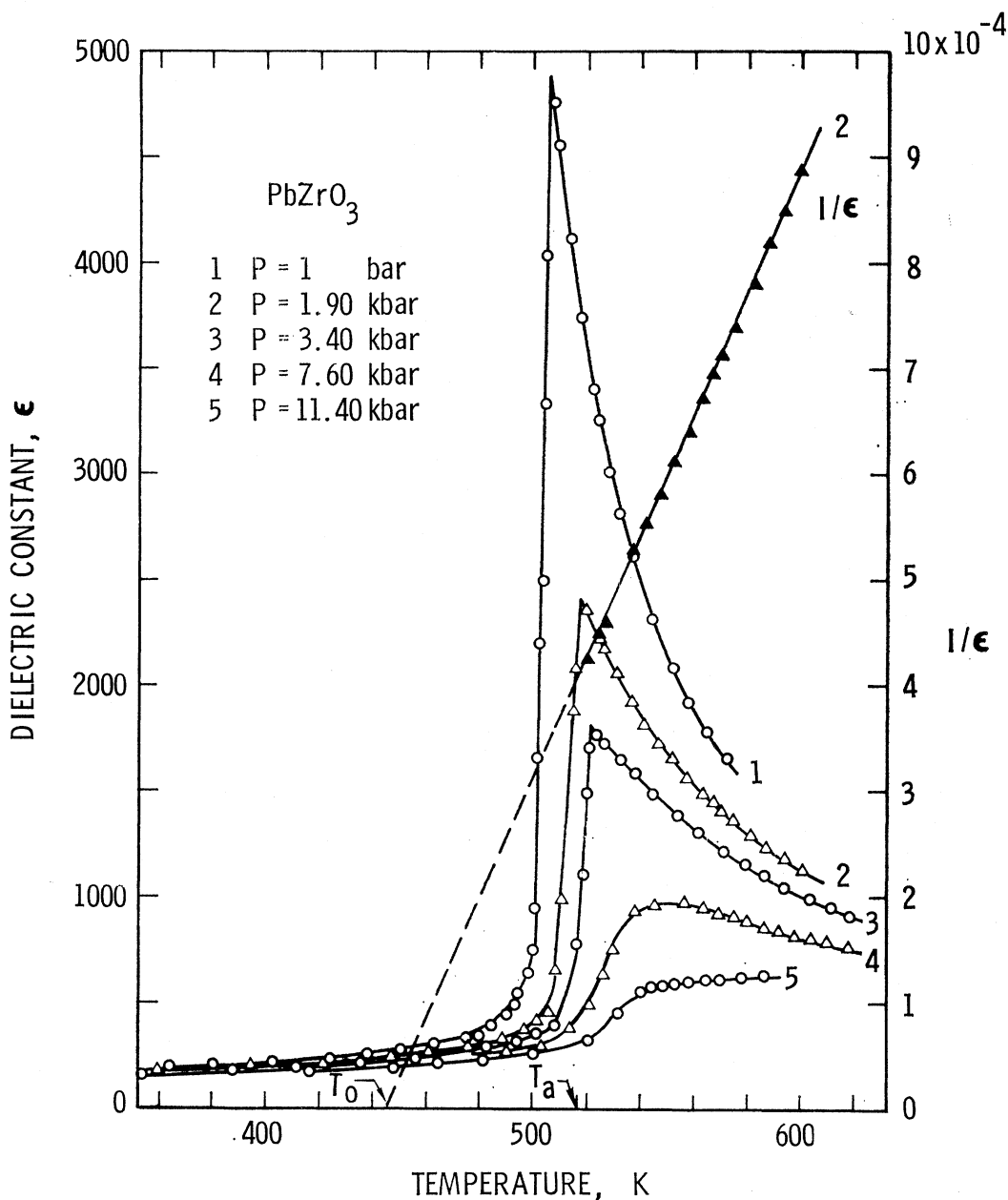


FIG. 1. Isobars of the temperature dependence (with increasing T) of the dielectric constant ϵ of PbZrO_3 . In the high-temperature paraelectric phase, ϵ obeys a Curie-Weiss law. The linear temperature variation of $1/\epsilon$, and the values of the Curie-Weiss temperature T_0 and the AFE-PE transition temperature T_a are indicated for the 1.90-kbar isobar.

More recently, however, Tennery¹⁸ and Goulpeau¹⁹ have observed the FE phase on both heating and cooling in "very pure" PbZrO_3 . On heating, this phase is stable over a 3–5°K range above $\sim 500^\circ\text{K}$, and on cooling it is stable over 10°K range. The volume changes at the AFE \rightarrow FE and FE \rightarrow PE transitions are +0.6 and -0.16% , respectively, according to

¹⁸ V. J. Tennery, *J. Am. Ceram. Soc.* **49**, 483 (1966).

¹⁹ L. Goulpeau, *Fiz. Tverd. Tela* **8**, 2469 (1966) [*Soviet Phys.—Solid State* **8**, 1970 (1967)].

Tennery, whereas Goulpeau's data yield +0.51 and -0.12% .

On the basis of the information given in Refs. 16–18, it is difficult to decide what causes the FE phase to be stable in some samples and absent in others. In the present work, where the samples were prepared from high-purity (>99.8%) starting materials, some evidence for the intermediate FE phase was noted in only one of the samples, but, as will be discussed later, this FE phase (when present) is "squeezed out" by pressure

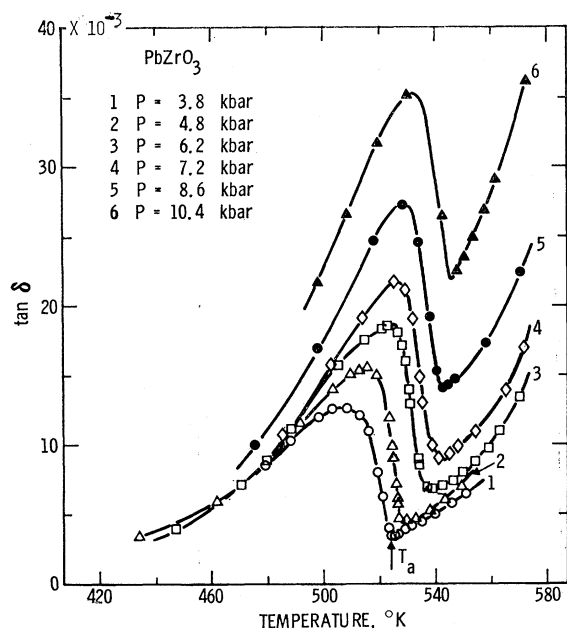


FIG. 2. Isobars of the temperature dependence of the dielectric loss, $\tan\delta$, of PbZrO_3 . A well-defined minimum is observed at the antiferroelectric transition temperature, T_a .

and only the AFE and PE phases are observed above ~ 1 kbar. It is the AFE-PE transition which is of most interest to us in this work.

PbHfO_3 exhibits two temperature-induced transitions at ~ 435 and $\sim 475^\circ\text{K}$.²⁰ The low-temperature phase is AFE and isomorphous with that of PbZrO_3 . The intermediate phase is tetragonal and is also AFE, but with a different type of dipole arrangement than the low-temperature orthorhombic phase. Above 475°K the crystal has the cubic perovskite structure.

Earlier pressure studies on PbZrO_3 and PbHfO_3 consist of a brief report by the author²¹ on the shift of the transition temperatures of both compounds obtained from measurements of the dielectric properties. Rapoport²² and more recently Reynaud *et al.*²³ obtained the shift of the transition temperature of PbZrO_3 from differential thermal analysis (DTA) measurements made at high pressure. The results of these earlier studies will be compared in Sec. V with results of the present work.

III. EXPERIMENTAL TECHNIQUES

The pressure measurements were made in a 30-kbar hydrostatic-pressure apparatus using a 50:50 mixture of normal pentane and isopentane as pressure fluid. A description of the apparatus and general experimental procedures including pressure calibration has been

²⁰ G. Shirane and R. Pepinsky, *Phys. Rev.* **91**, 812 (1953).

²¹ G. A. Samara, *Bull. Am. Ceram. Soc.* **44**, 638 (1965).

²² E. Rapoport, *Phys. Rev. Letters* **17**, 1097 (1966).

²³ R. Reynaud, Y. Fétiveau, M. Richard, and L. Eyraud, *Compt. Rend.* **267B**, 913 (1968).

presented elsewhere.²⁴ Pressure was measured with manganin gauges to an accuracy of $\pm 1\%$, and temperature changes were measured with Chromel-Alumel thermocouples to an accuracy of $\pm 0.1^\circ\text{K}$. The effect of pressure on the emf of these thermocouples is very small²⁵ over the range of pressures and temperatures of interest here and has been neglected. Sample capacitance and dielectric loss were measured at 100 kHz with a transformer ratio-arm bridge to an accuracy of $\pm 0.1\%$.

In the absence of single crystals of PbZrO_3 and PbHfO_3 , the measurements were made on polycrystalline specimens prepared by a hot pressing technique.²⁶ The specimens had densities $> 99.5\%$ of the theoretical values.²⁷ The sharpness of the observed transitions (see Sec. IV) are indicative of the homogeneity and good quality of the specimens. Typical sample dimensions were $(0.5-1.0)\text{ cm}^2 \times \sim 0.06\text{ cm}$ thick. Measurements were made on two or three samples cut from each specimen with good reproducibility among the results.

IV. EXPERIMENTAL RESULTS

A. PbZrO_3

Figure 1 shows the temperature dependence of the dielectric constant of a PbZrO_3 sample at various pressures. At 1 bar, the sample transformed from the AFE phase directly into the PE phase on heating with no evidence of an intermediate FE phase. The transition shifts to higher temperatures with increasing pressure, but the most pronounced pressure effects are the large decreases in both the sharpness of the transition and the dielectric anomaly associated with it. At pressures $> \sim 6$ kbar, it becomes difficult to determine the transition temperature T_a accurately from ϵ versus T isobars. Fortunately, however, T_a can be still determined up to ~ 12 kbar from dielectric loss ($\tan\delta$) versus T isobars which exhibit well-defined minima at T_a . Typical results are shown in Fig. 2. Above ~ 12 kbar the rapid increase of the conductivity of the material in the temperature range of interest reduces the $\tan\delta$ anomaly, and again it becomes difficult to determine T_a . All the observed changes are reversible on lowering the pressure.

B. PbHfO_3

Isobars of ϵ versus T for a PbHfO_3 sample are shown in Fig. 3. Qualitatively, the behavior is similar to that

²⁴ G. A. Samara, *J. Phys. Chem. Solids* **26**, 121 (1965).

²⁵ R. Hanneman and H. Strong, *J. Appl. Phys.* **36**, 523 (1965).

²⁶ G. H. Haertling, *Am. Ceram. Soc. Bull.* **42**, 679 (1963).

²⁷ For higher-porosity samples, the stress within the sample may be highly anisotropic even though the external applied stress is hydrostatic. This is due to the large difference between the compressibilities of the sample and the pores. Care must be exercised in interpreting results of pressure measurements on porous samples [see R. C. Wayne, G. A. Samara, and R. A. Lefever, *J. Appl. Phys.*, **41**, 633 (1970)].

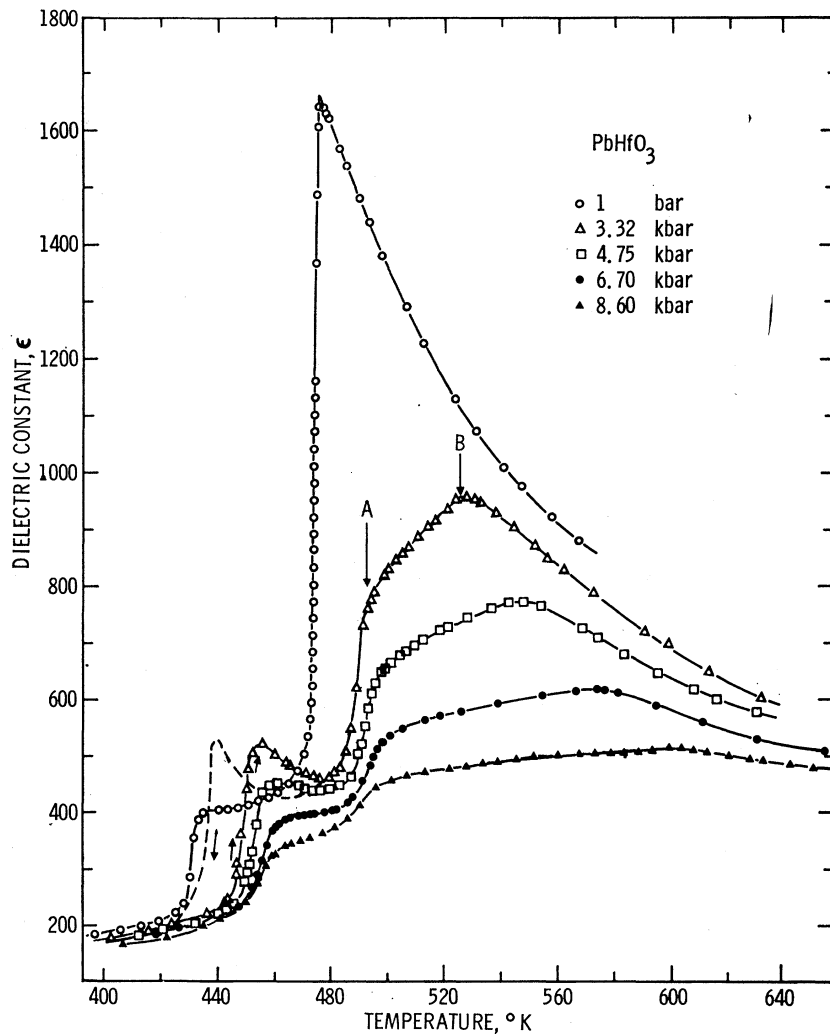


FIG. 3. Variation of the dielectric constant with temperature at various pressures for PbHfO₃. A large temperature hysteresis is observed at the lower transition as is illustrated for the 3.32-kbar isobar. A new phase lying between the arrows at A and B becomes stable at high pressure.

for PbZrO₃ in that pressure displaces the transitions to higher temperatures and there is a sharp reduction in the ϵ anomaly at the AFE-PE (upper) transition.

There are several noteworthy features of the results in Fig. 3. At 1 bar, the transitions were observed at 433 and 476°K with increasing temperature. These values, which were determined from both ϵ -versus- T and $\tan\delta$ -versus- T data, are in good agreement with the 434 and 477°K values reported by Goulpeau *et al.*,¹⁹ but the upper one is substantially lower than the early value of 488°K reported by Shirane and Pepinsky.²⁰ Both transitions are first-order with the lower exhibiting a 14°K temperature hysteresis between increasing and decreasing temperature cycles (as illustrated for the 3.32-kbar isobar in Fig. 3), whereas the upper transition has a negligible hysteresis. The present ϵ anomaly at the upper transition is about three times larger than that reported previously.²⁰

One of the more important features of the effects of pressure is the appearance of a new phase whose temperature range of stability increases with increasing

pressure.²⁸ This new phase, lying between the arrows at A and B in Fig. 3, is clearly defined from both ϵ -versus- T and $\tan\delta$ -versus- T data. At pressures >9 kbar, the anomalies in both ϵ and $\tan\delta$ become smeared out, and accurate determination of the various transition temperatures become difficult.

V. DISCUSSION

A. Transition Temperatures

1. PbZrO₃

Figure 4 shows the effect of pressure on the AFE \rightarrow PE transition temperature T_a for PbZrO₃, and compares the present results with earlier work. The shift is linear up to ~ 6 kbar with slope $dT_a/dP = 4.5 \pm 0.3^\circ\text{K/kbar}$. This value is in good agreement with the earlier value of $4.2 \pm 0.3^\circ\text{K/kbar}$ obtained by both the present author²¹ from dielectric constant measure-

²⁸ A brief account of this phase was given in G. A. Samara, *Phys. Letters* **30A**, 446 (1969).

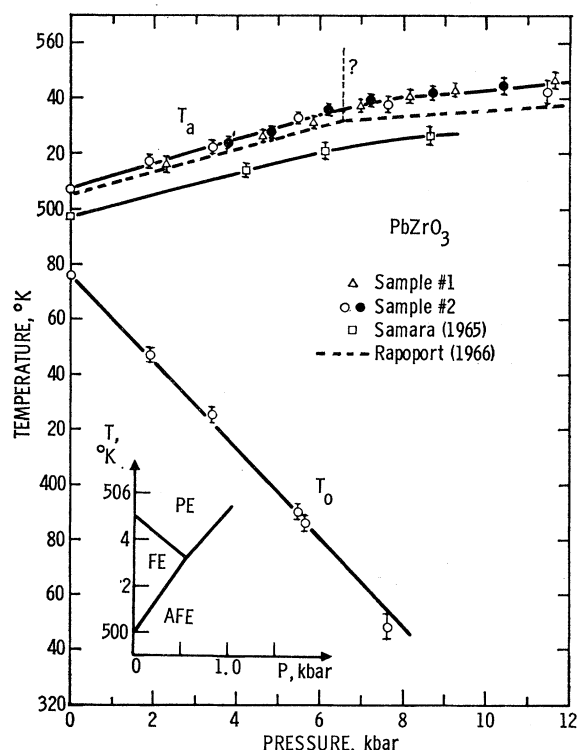


FIG. 4. The effects of pressure on the antiferroelectric transition temperature T_a and the Curie-Weiss temperature T_0 of PbZrO_3 . The error bars represent the total estimated experimental uncertainty. Insert shows that the intermediate FE phase, when present, vanishes above ~ 0.5 kbar.

ments and Rapoport²² from differential-thermal-analysis (DTA) measurements; however, it disagrees with the more recent value of $1.6 \pm 0.2^\circ\text{K}/\text{kbar}$ reported by Reynaud *et al.*²³ from DTA measurements to ~ 0.5 kbar. As will be shown below, this latter value is not consistent with that calculated from thermodynamic considerations.

Above ~ 6 kbar there is a marked decrease in the value of dT_a/dP . The present results indicate that the change in slope is continuous. Rapoport's data suggested a triple point in the P - T phase diagram at ~ 6.5 kbar, and thus the existence of another phase boundary as indicated schematically by the vertical dotted line in Fig. 4. In an effort to determine whether or not such a boundary occurs, measurements were made of ϵ and $\tan\delta$ versus pressure at temperatures $> 530^\circ\text{K}$, but no phase transitions were noted (see Fig. 5).

The $\text{AFE} \rightarrow \text{PE}$ transition in PbZrO_3 is a first-order transition, and the shift of T_a with pressure can be expected to obey the Clausius-Clapeyron equation

$$dT_a/dP = T_a \Delta V / L, \quad (5)$$

where ΔV is the volume change at the transition, and L is the latent heat. Precise determination of L is very difficult; however, since the transition is first-order, it can be assumed as a first approximation that most of the

measured transition heat Q (see Table I) comes from the latent heat, and one can therefore set $L \approx Q$. Using the values of ΔV and Q , given in Table I, Eq. (5) yields $dT_a/dP = 5.0 \pm 0.7^\circ\text{K}/\text{kbar}$, which is in reasonably good agreement with the experimental values.

It was mentioned earlier that there is evidence that an intermediate FE phase is observed in some samples of PbZrO_3 . Recent thermal expansion measurements^{18,19} have shown that discontinuous volume changes of $+(0.5$ to $0.6\%)$ and $-(0.12$ to $0.16\%)$ occur at the $\text{AFE} \rightarrow \text{FE}$ and $\text{FE} \rightarrow \text{PE}$ transitions, respectively. Substitution in Eq. (5) of these values of ΔV and of the values of Sawaguchi *et al.*,¹⁶ ~ 400 and ~ 200 cal/mole, respectively, for the transition energies, yields $dT/dP = +6.5 \pm 1^\circ\text{K}/\text{kbar}$ for the $\text{AFE} \rightarrow \text{FE}$ transition and $-3.6 \pm 0.6^\circ\text{K}/\text{kbar}$ for the $\text{FE} \rightarrow \text{PE}$ transition. Since the FE phase is usually observed over a very narrow temperature range of only a few degrees, these values show that the FE phase, when present, is "squeezed out" at pressures below 1 kbar, and only the AFE-PE transition is observed at higher pressures. This is illustrated in the insert in Fig. 4.

2. PbHfO_3

Fig. 6 shows the temperature-pressure phase diagram for PbHfO_3 . For convenience, the different phases are labeled α , β , γ , and δ , with decreasing temperature. The transition temperatures were determined from the anomalies in both ϵ and $\tan\delta$. For the γ - δ transition, the transition temperature is taken as the average of the $\gamma \rightarrow \delta$ and $\delta \rightarrow \gamma$ transition temperatures, the temperature hysteresis being initially $\sim 14^\circ\text{K}$ and decreases with pressure. There is negligible hysteresis at the other transitions. The initial slopes dT/dP of the various

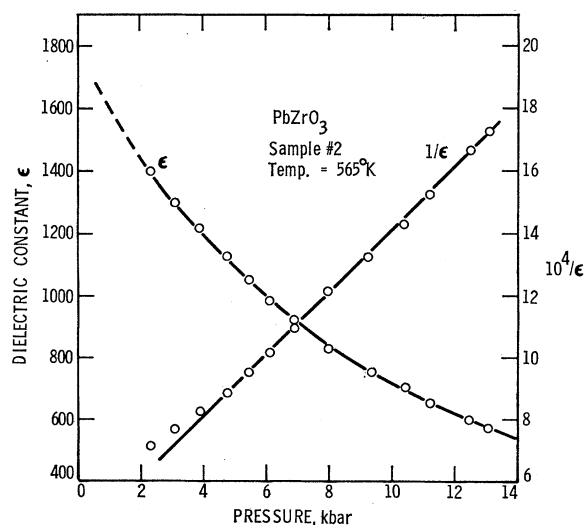


FIG. 5. The pressure dependence of the dielectric constant ϵ of PbZrO_3 in the cubic paraelectric phase. The linear variation of $1/\epsilon$ with pressure over a relatively wide pressure range is also shown.

phase boundaries in $^{\circ}\text{K}/\text{kbar}$ are 14.3 ± 1.0 for α - β , 5.0 ± 0.5 for β - γ , and 5.9 ± 0.6 for γ - δ .

Shirane and Pepinsky's data²⁰ have shown that at 1 bar there are discontinuous volume contractions of 0.16 \AA^3 and 0.27 \AA^3 at the $\alpha \rightarrow \gamma$ and $\gamma \rightarrow \delta$ transitions, respectively. The latent heats (or Q) apparently have not been measured. From the above value of ΔV and our measured value of dT/dP , Eq. (5) yields $L = 290 \pm 30$ cal/mole at the $\delta \rightarrow \gamma$ transition. This value of L is comparable to that observed for PbZrO_3 . Because of the appearance of the β phase under pressure, there are not sufficient volumetric data to calculate L for the other transitions.

The results in Fig. 6 indicate that at 1 bar and $\sim 475^{\circ}\text{K}$ the free energy of the β phase is comparable, but slightly higher than that of the γ phase, and that it is very sensitive to the unit cell volume. Although high-pressure x-ray and/or neutron-diffraction and other auxiliary measurements are needed to establish the exact nature of the new β phase, our present results indicate that this phase is also AFE. The evidence is based on polarization-versus-electric-field measurements which failed to reveal any definite evidence for ferroelectricity, and this is further supported by the increase in the $T_{\alpha-\beta}$ transition temperature with pressure. In the perovskites, with decreasing T , transitions to ferroelectric (FE) phases are accompanied by increases in unit cell volume, whereas transitions to AFE phases are accompanied by decreases in volume. As a result [see Eq. (5)], pressure lowers FE transition temperatures and raises AFE transition temperatures. Studies on a large number of FE and AFE perovskites, including PbZrO_3 and PbHfO_3 , have confirmed this observation.²⁹ The β phase in PbHfO_3 is definitely not related to the intermediate FE phase observed in PbZrO_3 . As discussed above, the PE \rightarrow FE transition in PbZrO_3 is accompanied by a volume expansion, and $T_{\text{PE-FE}}$ decreases with pressure, unlike $T_{\alpha-\beta}$ in PbHfO_3 .

B. Dielectric Properties and Lattice Dynamics

1. Curie-Weiss Behavior and Ferroelectric Mode

In the cubic paraelectric phase, the dielectric constants of PbZrO_3 and PbHfO_3 , measured at constant pressure, obey the Curie-Weiss law, Eq. (1), over wide temperature ranges (see Figs. 1 and 3). The 1 bar values of C and T_0 are given in Table II, which also shows values of these constants for BaTiO_3 and SrTiO_3 for comparison. Over the range of the measurements T_0 decreases linearly with pressure (see, e.g., Fig. 4), and values of dT_0/dP are given in Table II. The Curie constant C increases at a rate of $\sim 3\%/ \text{kbar}$ for PbZrO_3 and $< 1\%/ \text{kbar}$ for PbHfO_3 .

At constant temperature, the pressure variation of ϵ in the PE phase can be fairly well represented by the

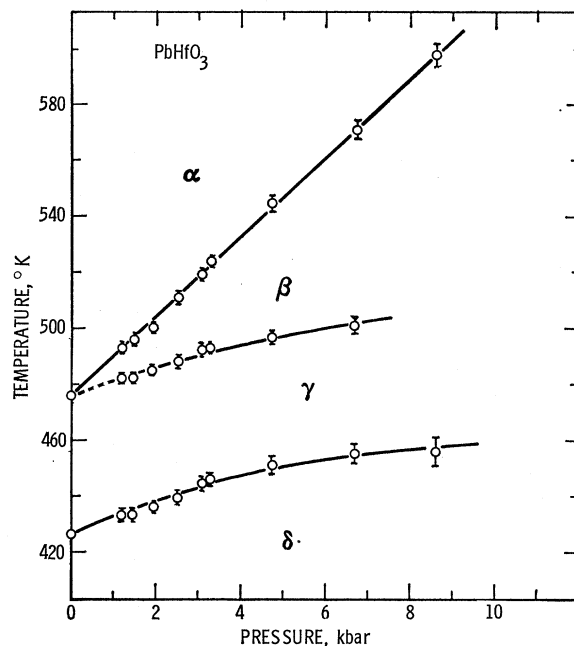


FIG. 6. The temperature-pressure phase diagram for PbHfO_3 . The β phase is induced by pressure. The error bars represent the total estimated experimental uncertainty. For the γ - δ transition, where there is a large temperature hysteresis (see Fig. 3), the transition temperature is taken as the average of the $\gamma \rightarrow \delta$ and $\delta \rightarrow \gamma$ values, and the error bars represent the uncertainty in this average value.

expression

$$\epsilon = C^*/(P - P_0), \quad (6)$$

where C^* and P_0 are constants. This is illustrated for PbZrO_3 in Fig. 5 and typical values of C^* and P_0 are given in Table II. It is seen that the C^* values are of the same magnitude as those found for BaTiO_3 and SrTiO_3 . The P_0 values depend, of course, on the substance and are strongly temperature-dependent. Equation (6) is found to hold²⁹ over a wide pressure range for most ferroelectrics in their PE phases.

The successful model theories of the dielectric properties of the perovskites start with the treatment of the static dielectric constant (ϵ) in the PE phase and its variation with temperature as conditions approach the transition temperature. It has become customary to discuss this temperature dependence of ϵ and the

TABLE II. Values for PbZrO_3 and PbHfO_3 of the Curie constant C , Curie-Weiss temperature T_0 , and its pressure derivative and of the constants C^* and P_0 which appear in Eq. (6). The corresponding values for BaTiO_3 and SrTiO_3 (taken from Ref. 30) are also listed for comparison.

Substance	C (10^5 °K)	T_0 (°K)	dT_0/dP (°K/kbar)	C^* (10^4 kbar)	P_0 (kbar)
PbZrO_3	1.60	475	-16.0 ± 0.5	1.0@564°K	-4.1@564°K
PbHfO_3	1.65	378	-10.0 ± 1.0	1.1@603°K	-12.8@603°K
BaTiO_3	1.5	380	-5.3 ± 0.6	2.8@296°K	18.0@296°K
SrTiO_3	0.83	36	~ -14	1.2@296°K	-40.3@296°K

²⁹ G. A. Samara, in *Advances in High Pressure Research*, edited by R. S. Bradley (Academic, New York, 1969), Vol. 3, Chap. 3.

ensuing transition to the FE state (a condition that does not quite obtain in PbZrO_3 and PbHfO_3 because of the condensation of the AFE mode) in terms of either of the following: (i) a polarization catastrophe whereby at the critical temperature the polarization becomes very large and the local field associated with it increases faster than the elastic restoring force, thus leading to an asymmetric distortion of the lattice, or (ii) a "soft" transverse optic (TO) phonon whose frequency $\rightarrow 0$ as $T \rightarrow T_0$ (see Sec. I). These two approaches are, in fact, two different ways of saying the same thing, and they are related via the Lyddane-Sachs-Teller relation.

In terms of the polarization catastrophe, the static and high-frequency dielectric constants are related via the local fields at the various lattice sites, to either macroscopic polarizabilities or to microscopic polarizabilities of the individual ions.²⁹⁻³¹ Using the resulting generalized Clausius-Mossotti relationship, measurements of the pressure and temperature dependences of the dielectric constants and of the compressibility and thermal expansion can be combined to evaluate the explicit volume V and temperature dependences of the polarizabilities. Following earlier^{30,31} procedures, we find³² for PbZrO_3 and PbHfO_3 (as is true for BaTiO_3 and SrTiO_3) that it is the explicit T dependence of the lattice (or infrared) polarizability (α_{ir}), i.e., $(\partial\alpha_{\text{ir}}/\partial T)_V$, which makes the dominant contribution to the T dependence of ϵ at constant pressure, i.e., $(\partial\epsilon/\partial T)_P$. This explicit T dependence of α_{ir} arises from anharmonic terms in the potential energy of the crystal, and it leads directly to the T -dependence of the phonon frequencies—hence the question of "soft" TO phonons as described in Sec. I.

From Eq. (3b) it is seen that the pressure dependence of ϵ reflects that of ω_f^2 . In particular, if it is assumed that the quantity A is independent of pressure, then the observed linear increase of $1/\epsilon$ with pressure (at constant T) in the PE phase (Eq. 6) implies that ω_f^2 should also increase linearly with pressure as

$$\omega_f^2 = K^*(P - P_0), \quad (7)$$

where K^* and P_0 are constants.

Although at present there are no direct measurements of ω_f versus pressure for either PbZrO_3 and PbHfO_3 or any other perovskites, some supporting evidence for Eq. (7) has come from electrical conductivity measurements. Wemple *et al.*³³ measured the effect of pressure on the conductivity σ of several perovskites in their cubic PE phases and observed a large increase in σ similar to that for $1/\epsilon$ versus P . This increase in σ could

not be explained on the basis of repopulation effects or change in the effective mass and was thus attributed to a strongly pressure-dependent electron relaxation time. Lattice scattering is dominant in these materials, and this scattering is attributed mainly to the long-wavelength TO mode, i.e., the FE mode. In the perovskites, the electron mean free path is of the order of a few angstroms (i.e., a lattice parameter), so that electrons can be scattered by the local distortion of the unit cell produced by the FE mode.

The results of Wemple *et al.* showed that the electron mobility μ_e is related to ϵ by $\mu_e \propto [(1/\epsilon) + \text{constant}]$, and it thus follows that

$$\sigma \propto \mu_e \propto \omega_f^2. \quad (8)$$

The increase, or "hardening," of ω_f with pressure can be qualitatively understood in the following way. The FE mode in the perovskites corresponds³⁴ to the vibration of the positively charged B ion in the ABO_3 structure against the rest of the lattice (primarily the negatively charged oxygen octahedron). It is reasonable to expect the restoring force, and thus the frequency, for this vibration to increase with decreasing interatomic distances (i.e., increasing pressure). Alternatively, ω_f^2 can be schematically expressed as $\omega_f^2 \propto (\text{short-range forces}) - (\text{Coulomb forces})$. Since the short-range forces are expected to be much more strongly dependent on interatomic distances than the long-range Coulomb forces, the short-range term increases faster than the Coulomb term, thus leading to an increase in ω_f . To establish theoretically the indicated pressure dependence of ω_f , namely, $\omega_f \propto P^{1/2}$, one needs to determine the pressure dependences of the various force constants and other parameters in the shell model or any other dynamical model of the lattice. That is a formidable task.

2. Antiferroelectric Mode(s)

According to Eq. (4), the increase of the AFE transition temperature T_a with pressure shows that the AFE mode "softens" with decreasing volume. In the absence of experimental data on the phonon dispersion relations and their T dependence in PbZrO_3 , some insight into the nature of the AFE mode can be gained by examining the displacements of the various ions which occur at the PE \rightarrow AFE transition. The basic idea here is that if one of the modes has a much lower frequency than the others, then the displacement associated with this mode would be expected to be large and predominate. This follows from the relationship³⁵

$$\omega(\mathbf{q}, j) \propto 1/\langle Q(\mathbf{q}, j) \rangle, \quad (9)$$

³⁰ G. A. Samara, Phys. Rev. **151**, 378 (1966).

³¹ W. N. Lawless and H. Gränicher, Phys. Rev. **157**, 440 (1967).

³² The compressibilities of PbZrO_3 and PbHfO_3 apparently have not been measured. For the present calculation it was assumed that these compressibilities are comparable to those for BaTiO_3 and SrTiO_3 given in Ref. 29.

³³ S. H. Wemple, M. DiDomenico, Jr., and A. Jayaraman, Phys. Rev. **180**, 547 (1969); Phys. Rev. Letters **17**, 142 (1966).

³⁴ G. Shirane, in Proceedings of the Second International Meeting of Ferroelectricity, Kyoto, Japan, 1969 [J. Phys. Soc. Japan (to be published)].

³⁵ See, e.g., P. C. Kwok and P. B. Miller, Phys. Rev. **151**, 387 (1966).

where $\langle Q(\mathbf{q}, j) \rangle$ is the thermal expectation value of the normal coordinate which is related to the displacement $[u(lk)]$ of the k th atom in the l th unit cell from the equilibrium position in the PE phase. In PbZrO_3 , the transition to the orthorhombic AFE phase involves primarily antiparallel displacements of the Pb ions along one of the cubic $\langle 110 \rangle$ directions and antiparallel displacements of the oxygen ions in the (001) plane.¹⁵ The displacements at the various transitions in PbHfO_3 are not well known at present.

Cochran and Zia³ have recently examined the measured displacements in PbZrO_3 , and they find that several modes may be involved in the cubic (PE) \rightarrow orthorhombic (AFE) transition. Using the notation (\mathbf{q}, R) to identify a wave vector \mathbf{q} (in units of $2\pi/a$) for which the pattern of displacements is described by the irreducible representation R , they find that at least four values of (\mathbf{q}, R) are present in the orthorhombic phase³⁶: $(000, \Gamma_{15})$, $(\frac{1}{4} \frac{1}{4} 0, \Sigma_3)$, $(\frac{1}{2} \frac{1}{2} 0, M'_5)$, and $(\frac{1}{2} \frac{1}{2} \frac{1}{2}, \Gamma_{25})$. The first of these is associated with the $\mathbf{q} = 0$ FE mode. The fact that the transition involves a change in the crystal involving more than one irreducible representation is consistent with the transition being first-order.¹⁴

Without further evidence, it is difficult to assess the relative contribution of each of the above modes to the transition. However, there are two observations which may have important bearing on this point. First, the atomic displacements associated with the $(\frac{1}{2} \frac{1}{2} 0, M'_5)$ mode are very small³ in PbZrO_3 , and Cowley's⁹ theoretical treatment of the lattice dynamics of SrTiO_3 has shown that $\omega_{M'_5}$ is not strongly dependent on temperature. These features suggest that this mode is not very important in the PbZrO_3 transition. Secondly, the softening of the frequency of the $(\frac{1}{2} \frac{1}{2} \frac{1}{2}, \Gamma_{25})$ mode has recently been experimentally shown^{1,2,4} to be the cause of the cubic \rightarrow distorted perovskite structure transitions in SrTiO_3 (110°K), KMnF_3 (184°K), and LaAlO_3 (800°K). Since the displacements associated with this mode are fairly large in PbZrO_3 , one is tempted to suspect that Γ_{25} may play the key role in this transition also; however, in the presence of large displacements associated with the $(\frac{1}{4} \frac{1}{4} 0, \Sigma_3)$ mode³ there are no strong *a priori* justifications for doing so. In fact, since the unit cell appears to be enlarged (or the Brillouin zone decreased) by a factor of 8 at the cubic \rightarrow orthorhombic transition, the softening of ω_{Σ_3} may be the primary cause for the transition in PbZrO_3 . A study of the T dependence of the phonon dispersion relations in PbZrO_3 (and in PbHfO_3), when single crystals become available, should be most revealing. The question of whether or not the *simultaneous* softening and con-

densation of all the indicated modes do occur at the transition is of particular interest.

Finally, the experimental results (Fig. 1) show that with increasing pressure the first-order AFE transition in PbZrO_3 (and similarly for the transitions in PbHfO_3 , Fig. 3), acquires the characteristics of a second-order transition. This is evidenced by the decrease in the sharpness of the transition and is further supported by Rapoport's²² differential thermal analysis measurements which indicate that the latent heat at the transition decreases rapidly with pressure. At atmospheric pressure, the soft AFE mode (or modes) is strongly coupled to the macroscopic strain parameters, and evidently this coupling becomes weaker at high pressure. Again, without knowledge of the dispersion relations it is difficult to say much about the nature of this coupling. However, it is of interest to note that Axe *et al.*³⁷ find that under certain conditions strong harmonic coupling between optic- and acoustic-like excitations can obtain in perovskites. They suggest that such coupling can lead to an instability in a mode with mixed acoustic-optic character and nonzero (middle of the zone) wave vector, giving rise to an AFE phase. The $(\frac{1}{4} \frac{1}{4} 0, \Sigma_3)$ mode in PbZrO_3 may well be a mode of this type.

VI. SUMMARY AND CONCLUSIONS

In this work the effects of temperature and hydrostatic pressure on the dielectric properties and phase transitions of PbZrO_3 and PbHfO_3 were investigated. The results show that in both crystals there are two independent low-frequency (nearly degenerate at 1 bar) temperature-dependent lattice vibrational modes: a FE mode which determines the Curie-Weiss behavior of the static dielectric constant ϵ in the PE phase, and an AFE mode(s) which causes the PE-AFE transition. With increasing pressure, the frequency of the FE mode increases (corresponding to a decrease in the Curie-Weiss temperature), whereas the frequency of the AFE mode decreases (corresponding to an increase in the AFE-PE transition temperature). As a result, the large anomaly in ϵ at the transition decreases sharply. The nature of the AFE mode in PbZrO_3 was discussed briefly.

The intermediate FE phase observed over a narrow temperature range between the AFE and PE phases in *some* samples of PbZrO_3 vanishes at pressures above ~ 1 kbar.

In addition to the two AFE phases which are stable in PbHfO_3 at 1 bar, a third AFE phase is induced in this crystal by the application of pressure. The temperature range of stability of this phase increases rapidly with pressure. All the AFE transition temperatures in PbHfO_3 increase with pressure corresponding to the softening of their respective AFE modes.

³⁶ According to the theoretical analysis of Miller and Kwok (Ref. 14), two other modes having $\mathbf{q} = (0 0 \frac{1}{2})$ and $(\frac{1}{4} \frac{1}{4} \frac{1}{2})$ should be present. The fact that the displacements associated with these modes are not detectable indicates that the corresponding frequencies are too high, and, thus, these two modes most likely do not play a key role in the transition.

³⁷ J. D. Axe, J. Harada, and G. Shirane, Phys. Rev. (to be published).

With increasing pressure the first-order AFE-PE transitions in PbZrO_3 and PbHfO_3 acquire the characteristics of second-order transitions. These effects undoubtedly reflect important pressure-induced changes in the ionic displacements accompanying these transitions.

ACKNOWLEDGMENTS

I wish to thank my colleagues G. H. Haertling and C. A. Hall for providing the specimens, and W. L. Chrisman for technical assistance.

Low-Temperature Behavior of a Pure Dipole-Dipole System

PAUL H. E. MEIJER

Catholic University of America, Washington, D. C. 20017

and

National Bureau of Standards, Washington, D. C. 20234

AND

DAVID J. O'KEEFE

Naval Ordnance Laboratory, White Oak, Maryland

(Received 1 December 1969)

The Van Vleck moment expansion is applied to a pure dipole system. On the basis of the long-range nature of the forces, sequences of diagrams are selected that give the dominant contributions in the lattice sums. A selection of diagrams contributing to the entropy and susceptibility is displayed. There are three different summations to be performed for each type of diagram: the trace over the spin variables, the lattice summation, and the summation over the Cartesian coordinates. The second was performed on a computer, and the last is obtained by means of the Kramers-Wannier diagonalization. In order, to obtain the contributions of diagrams of higher order, a Fourier transform is employed. The calculations are performed for cerous magnesium nitrate using a g factor that is zero along the c axis. The results are compared with experiments. The susceptibility χ was calculated for a uniform and for a nonuniform field, and it is suggested that the critical temperature is determined by the infinity of $\chi(q)$ for $q \neq 0$, rather than by that of $\chi(0)$.

I. GENERAL CONSIDERATIONS

IN order to predict a critical point T_c and the state of magnetization below T_c , one needs a complete set of parameters to describe the magnetic system. They are:

(a) The lattice structure—the type of crystal structure and the actual lengths and orientations of the lattice vectors \mathbf{a} , \mathbf{b} , \mathbf{c} , as well as the parameters u , v , etc., describing the atoms in the unit cell, if more than one.

(b) The g factors, more specifically the tensors, one for each atom per unit cell.

(c) The interaction as a function of the relative distance $J(r_{ij})$, which in general can be of the tensorial type, i.e., not necessarily dependent on the distance only.

Suppose all these data were available, how can we go about determining the critical temperature?

Before answering this question let us take a look at the availability of the data just mentioned. As far as (a) is concerned a sufficient amount of good data is usually available from x-ray work. The only practical trouble is that the lattice parameters are not always determined at the temperature range one is interested in and although the changes at low temperatures are usually minute, the coefficients to be calculated later are very sensitive to the values of the parameters.

The g factors are also sufficiently known in most cases. The values of g_{\perp} and g_{\parallel} as well as the axis with respect to which they are parallel and perpendicular are very often known from paramagnetic resonance experiments in diluted crystals.

The third quest for data, the interaction as a function of the relative distance is the weakest link in the chain. Although recently a number of successful experiments have been performed to determine the nearest- and next-nearest-neighbor interactions between paramagnetic ions from satellite lines in a number of moderately diluted crystals,¹ the data are far from complete. There is one exception, however, the salts in which the dipole-dipole interaction is dominant. It is reasonable to assume that the permeability of an insulator is the same as that of the vacuum and although occasionally pseudo-dipole forces have been proposed² one feels that the use of the “free” dipole-dipole interaction is a good description in cases where the exchange forces seem to be weak. It is much less clear that higher multipole forces should not be taken into account.

The attraction to study the case of dominant dipolar forces as a challenge for the theory is clear: Here one

¹ See, for instance, M. T. Hutchings, R. J. Birgeneau, and W. P. Wolf, *Phys. Rev.* **168**, 1026 (1968); **179**, 275 (1969).

² J. H. Van Vleck and J. van Kranendonck, *Rev. Mod. Phys.* **30**, 1, (1958).